Interaction of 3,4-Dienoyl-CoA Thioesters with Medium Chain Acyl-CoA Dehydrogenase: Stereochemistry of Inactivation of a Flavoenzyme†

Wenzhong Wang,‡,§ Zhuji Fu,§,|| Jing Zhi Zhou,‡ Jung-Ja P. Kim,*,|| and Colin Thorpe*,‡

Department of Chemistry and Biochemistry, University of Delaware, Newark, Delaware 19716, and Department of Biochemistry, Medical College of Wisconsin, Milwaukee, Wisconsin 53226

Received May 14, 2001; Revised Manuscript Received August 14, 2001

ABSTRACT: The medium chain acyl-CoA dehydrogenase is rapidly inhibited by racemic 3,4-dienoyl-CoA derivatives with a stoichiometry of two molecules of racemate per enzyme flavin. Synthesis of *R*- and *S*-3,4-decadienoyl-CoA shows that the *R*-enantiomer is a potent, stoichiometric, inhibitor of the enzyme. α-Proton abstraction yields an enolate to oxidized flavin charge-transfer intermediate prior to adduct formation. The crystal structure of the reduced, inactive enzyme shows a single covalent bond linking the C-4 carbon of the 2,4-dienoyl-CoA moiety and the N5 locus of reduced flavin. The kinetics of reversal of adduct formation by release of the conjugated 2,4-diene were evaluated as a function of both acyl chain length and truncation of the CoA moiety. The adduct is most stable with medium chain length allenic inhibitors. However, the adducts with *R*-3,4-decadienoyl-pantetheine and -*N*-acetylcysteamine are some 9- and >100-fold more kinetically stable than the full-length CoA thioester. Crystal structures of these reduced enzyme species, determined to 2.4 Å, suggest that the placement of H-bonds to the inhibitor carbonyl oxygen and the positioning of the catalytic base are important determinants of adduct stability. The *S*-3,4-decadienoyl-CoA is not a significant inhibitor of the medium chain dehydrogenase and does not form a detectable flavin adduct. However, the *S*-isomer is rapidly isomerized to the trans-trans-2,4-conjugated diene. Protein modeling studies suggest that the *S*-enantiomer cannot approach close enough to the isoalloxazine ring to form a flavin adduct, but can be facilely reprotonated by the catalytic base. These studies show that truncation of CoA thioesters may allow the design of unexpectedly potent lipophilic inhibitors of fatty acid oxidation.

Short, medium, long, and very long chain acyl-CoA dehydrogenases participate in mitochondrial fatty acid oxidation, with conversion of their straight chain acyl-CoA substrates to the corresponding enoyl-CoA derivatives. Mechanistic studies, primarily with the medium chain acyl-CoA dehydrogenase, suggest that α-proton abstraction is concerted with transfer of the *pro-R* β-hydrogen to the N5 position of the isoalloxazine ring as a hydride equivalent (Scheme 1) (*1*−*6*). The resulting air-stable complexes between reduced flavin and tightly bound enoyl-CoA products are then reoxidized by two molecules of electron-transferring flavoprotein in successive one-electron steps (*7*−*10*).

A number of mechanism-based inhibitors of the acyl-CoA dehydrogenases have been described. Both 3- and 2-alkynoyl-CoA derivatives attack the protein moiety of the oxidized enzyme after base-catalyzed abstraction of either α- (*3, 11, 12*) or γ-protons (*13*−*15*), respectively. GLU376 is the target of inactivation of the medium chain acyl-CoA dehydrogenase by 2-octynoyl-CoA, and the initial suggestion that this residue may be the catalytic base (*13, 14*) was confirmed by crystallography (*16, 17*) and mutagenesis (*18*). 5,6-Dichloro-4-thia-5-hexenoyl-CoA is also activated by the medium chain dehydrogenase (*19, 20*) with concomitant covalent modification of GLU376 (J. F. Baker-Malcolm, J.-J. P. Kim, and C. Thorpe, unpublished observations).

Scheme 1

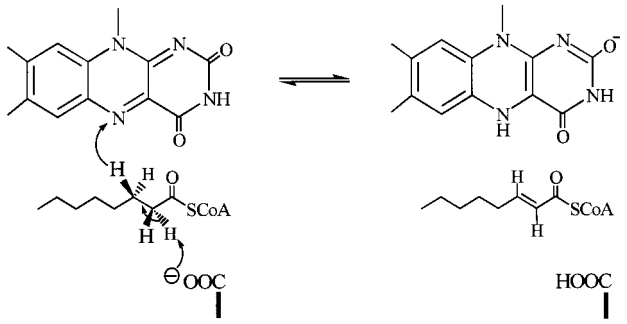

In contrast, several thioesters target the flavin prosthetic group of the dehydrogenase, yielding an enzyme-bound reduced FAD derivative (*21*−*28*). One of these, methylenecyclopropylacetyl-CoA (MCPA-CoA;[1] Chart 1, compound **1**), is formed during the metabolism of the toxic amino

† This work was supported in part by NIH Grants GM26643 (C.T.) and GM29076 (J.-J.P.K.).

* To whom correspondence should be addressed. C.T.: telephone, 302-831-2689; fax, -6335; e-mail, cthorpe@udel.edu. J.-J.P.K.: telephone, 414-456-8479; fax, -6510; e-mail, jjkim@post.its.mcw.edu.

‡ University of Delaware.

§ These authors contributed equally to the work.

|| Medical College of Wisconsin.

[1] Abbreviations: MCPA-CoA, methylenecyclopropylacetyl-CoA; DTNB, 5,5′-dithiobis(2-nitrobenzoic acid); NOE, nuclear Overhauser effect; COSY, correlation spectroscopy.

10.1021/bi0109818 CCC: $20.00
Published on Web 09/20/2001

Chart 1

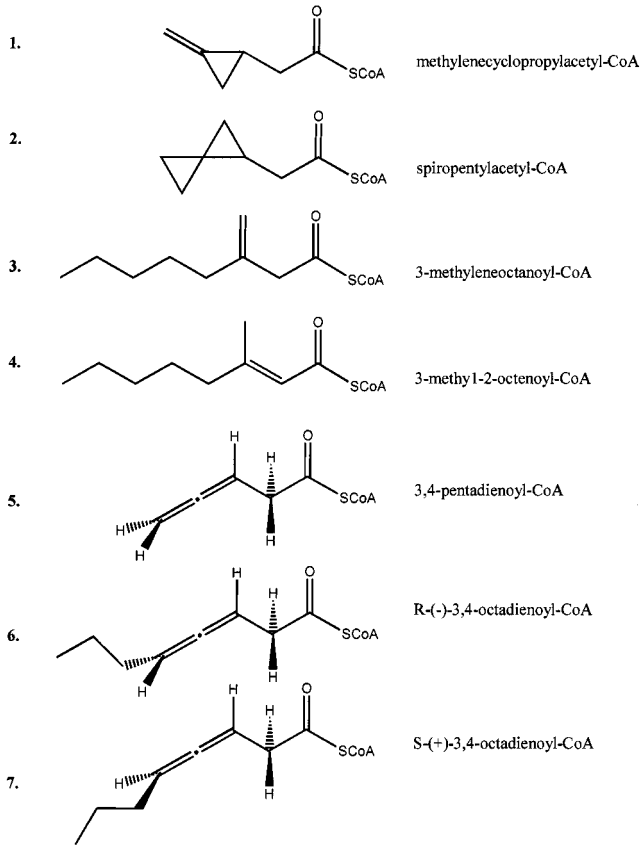

acid methylenecyclopropylalanine (hypoglycin A) found in unripe ackee fruit (*29*). After an initial α-proton abstraction step (*27*, *28*, *30*), MCPA-CoA treatment yields a stable reduced flavin adduct that cannot be reversed by a large excess of normal substrate. Strong evidence for the involvement of radical intermediates during inactivation has been obtained, although the structure, or structures, of the primary reduced flavin species on the enzyme remains to be fully elucidated (*23*, *25*, *27*, *28*, *30*) (P. Hubbard, H.-W. Liu, and J.-J. P. Kim, unpublished observations). A structurally related compound, spiropentylacetyl-CoA (compound **2**, Chart 1), inhibits short and medium chain acyl-CoA dehydrogenases with a component of irreversible inactivation and bleaching of the flavin chromophore (*23*, *31*). The short chain acyl-CoA dehydrogenase is also irreversibly inhibited by another cyclic thioester, cyclobutylacetyl-CoA, with bleaching of the flavin (*24*).

In contrast to these irreversible inhibitors, we recently reported an interesting class of inhibitors which form reversible reduced flavin adducts (*22*). Compounds **3** and **4** (Chart 1) are activated by α- and γ-proton, abstraction, respectively to form the same resonance-stabilized anion and, ultimately, the same reduced flavin species. Compound **3** is a particularly potent inhibitor both thermodynamically and kinetically (*22*).

This work shows that compound **5** in Chart 1 is the prototype for a distinct class of reversible inhibitors which target the flavin prosthetic group of the medium chain dehydrogenase. Ghisla and colleagues observed that addition of 1 equiv of 3,4-pentadienoyl-CoA leads to rapid reversible formation of a spectrum typical of an N5-reduced flavin adduct (via step k_2/k_{-2} in Scheme 2) (*32*). This species is

Scheme 2

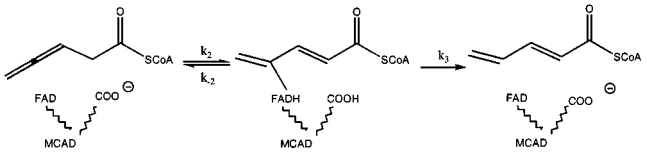

enzymatically inactive, but activity can be readily recovered by displacing the allene from the oxidized enzyme (step k_{-2}) with the tight binding substrate octanoyl-CoA (*32*). In the absence of displacing ligand, the reduced flavin adduct decomposes via k_3 with a half-life of 75 min, yielding oxidized flavin and the thermodynamically more stable conjugated isomer 2,4-pentadienoyl-CoA (*32*).

One object of the present work was to examine whether more potent inhibitors of the medium chain dehydrogenase could be synthesized with alkyl substituents at the terminal C-5 methylene position. However, substitution at C-5 in these allenes creates a new chiral center (for illustration, see *R*- and *S*-3,4-octadienoyl-CoA derivatives; Chart 1, compounds **6** and **7**). This work shows that these two isomers are processed differently by the dehydrogenase: one is a potent mechanism-based inactivator, the other an isomerase substrate of the enzyme. Further, the kinetic stability associated with an appropriately sized alkyl substituent at C-5 affords the opportunity to determine the crystal structure of a flavin adduct species. Two other notable aspects emerge from this work. Rapid reaction studies show, for the first time with the acyl-CoA dehydrogenase, an enolate intermediate prior to reduction of the flavin. In contrast, reduction of the flavin with normal substrates is concerted (see earlier). Second, pantetheine thioesters are, somewhat paradoxically, more potent inhibitors of the dehydrogenase than their full-length CoA counterparts. This suggests that membrane-permeant direct inhibitors of fatty acid oxidation might be designed.

MATERIALS AND METHODS

Materials. Medium chain acyl-CoA dehydrogenase was purified from pig kidney as described previously (*33*). Porcine liver esterase (EC 3.1.1.1), CoASH (lithium salt), D-pantethine, and 5,5′-dithiobis(2-nitrobenzoic acid) were obtained from Sigma. *E*,*E*-2,4-Hexadienoic acid, *E*,*E*-2,4-heptadienal, sorbic acid, racemic and chiral *R*- and *S*-1-octyn-3-ol, *N*-acetylcysteamine, ferrocenium hexafluorophosphate, and sinapinic acid were purchased from Aldrich. Sodium borohydride, monobasic potassium phosphate, diethyl ether, methyl *tert*-butyl ether, methanol, trifluoroacetic acid, and acetonitrile were from Fisher. *E*,*E*-2,4-Octadienal and *E*,*E*-2,4-dodecadienal were from Alfa and K & K Laboratories, respectively. D_2O was from Cambridge Isotope Labs.

General. Throughout this paper, the term equivalent represents the total amount of thioester (enantiomer or racemate) added per flavin. All concentrations of enzyme refer to active sites using an extinction coefficient of 15.4 mM^{-1} cm^{-1} at 446 nm (*34*). Unless otherwise stated, buffers were 50 mM potassium phosphate, pH 7.6, containing 0.3 mM EDTA, and experiments were conducted at 25 °C. Assays of the medium chain dehydrogenase were as described previously (*35*). Static spectrophotometry and rapid-reaction spectrophotometry were performed as before (*36*).

NMR spectra were recorded using either Bruker AC250 or Bruker DRX400 systems. Chemical shifts were referenced to a tetramethylsilane standard, or to the solvent resonances.

Synthesis of Racemic 3,4-Dienoic Acids. Dienals were oxidized by silver oxide to give the corresponding dienoic acids (*37*). The resulting acids were photoisomerized with a Hanovia L 450-W high-pressure mercury lamp to give racemic 3,4-dienoic acids as described by Crowley (*38*). Alternatively, methyl esters were synthesized from racemic precursors by the orthoester Claisen rearrangement (*39*) described below.

Synthesis of Chiral 3,4-Decadienoic Acids. R(−)- and *S*(+)-1-octyn-3-ols were the precursors for *R*(−)- and *S*(+)-methyl decadienoates, respectively (*39*). Each octynol (1.0 g) was mixed with propionic acid (40 mg) and trimethyl orthoacetate (7.6 g) and refluxed under nitrogen at 105 °C for 6 h. After completion of the reaction (TLC: using methanol/ethyl acetate 1:1 v/v; detection by iodine vapor), excess trimethyl orthoacetate was removed by distillation at 120 °C. The residue (1.68 g) was stirred for 30 min with 2 mL of 0.5 M H_2SO_4 and extracted with three 5 mL aliquots of ether. The extract was dried over anhydrous magnesium sulfate and the ether evaporated to yield 1.30 g of a pale yellow ester. The product was characterized by proton NMR in deuteriochloroform: -*O*-methyl, 3.75 ppm (s, 3H); C-2, 3.02 ppm (m, 2H); C-3 and C-5, 5.20 ppm (br, 2H); C-6, 1.95 ppm (m, 2H), and C-7, -8, and -9, 1.2−1.4 ppm (br, 6H). The optical rotations for *R*(−)- and *S*(+)-methyl esters in diethyl ether were $[\alpha]^{22}_D = -37.3°$ and +38.2°, respectively. A portion of the ester (0.45 g) was hydrolyzed by 200 units of porcine liver esterase (*40*) in 30 mL of 250 mM phosphate buffer, pH 7.0. The mixture was stirred vigorously at room temperature for 72 h in a closed flask under nitrogen, then acidified to pH 2 with HCl, and finally extracted with three 15 mL aliquots of ether. The extractions were pooled, and the ether was removed by rotary evaporation. The residue was washed with three 15 mL aliquots of 250 mM sodium bicarbonate solution (pH adjusted to 8), and unhydrolyzed ester was removed by ether extractions. The aqueous layer was brought to pH 2 with HCl and extracted with ether as before. The extract was dried and recovered to yield approximately 0.15 g of acid. Proton NMR showed the disappearance of the methoxy resonance and the emergence of a broad carboxylic acid resonance at 9 ppm. The acid preparations showed $[\alpha]^{22}_D = -57.7°$ and +60.1° for *R*- and *S*-isomers, respectively.

Preparation of 3,4-Allenic Thioesters. The allenoyl-CoA thioesters were synthesized by the mixed anhydride method (*41*) with minor modifications. Thus, 36.3 μmol of allenic acid, 36.3 μmol of isobutyl chloroformate, and 33.0 μmol of dry triethylamine were mixed in 2.0 mL of dry tetrahydrofuran and stirred for 10 min at room temperature. CoASH (24.2 μmol in 1.5 mL of 250 mM phosphate buffer, pH 8.2) was added and the mixture stirred under nitrogen for 20 min. The solution was then acidified to pH 5 with glacial acetic acid and the mixture then extracted with diethyl ether. The remaining aqueous layer was purified by HPLC as before (*42*). Here, a shallow gradient of methanol and 25 mM potassium phosphate, pH 5.3, was used to resolve the 3,4-allene from a small amount of 2,4-dienoyl-CoA contaminant. A typical elution program for 3,4-decadienoyl-CoA was the following: 1.5 min, phosphate buffer alone; 1.5−3.5 min, linear gradient to 65% methanol; 3.5−12 min, linear gradient to 66% methanol; 12−15 min, linear gradient to 80% methanol; 15−20 min, linear gradient to 100% phosphate buffer. Here, 3,4-decadienoyl-CoA eluted at 13.7 min. The gradient was tailored to the varying chain lengths of thioesters synthesized in this work. All resulting 3,4-allenic CoA thioesters were quantitated using an extinction coefficient of 16 mM^{-1} cm^{-1} at 260 nm. The 3,4-decadienoyl-CoA showed the expected proton NMR spectrum.

The above protocol was adapted to synthesize the corresponding pantetheine and *N*-acetylcysteamine thioesters. First, pantetheine was prepared using sodium borohydride reduction of D-pantethine as described earlier (*11*). The reaction was quenched with acetone, and the pH was carefully adjusted to 8.2. The reduced preparation was stored in aliquots at −70 °C and standardized with DTNB before use. With either pantetheine or *N*-acetylcysteamine, the thioesterification reaction mixture was not adjusted to pH 5.3, but extracted with three 4 mL ether aliquots. The extracts were combined, dried over anhydrous magnesium sulfate, and stripped of solvent. The thioesters were dissolved in 20% acetonitrile and purified by HPLC using a water/acetonitrile gradient followed at 234 nm. Both thioesters were quantitated using an extinction coefficient of 3.8 mM^{-1} cm^{-1}.

Kinetic Stability of Adducts Formed between 3,4-Dienoyl-CoA Derivatives and the Medium Chain Acyl-CoA Dehydrogenase. A solution of acyl-CoA dehydrogenase (9.5 μM in 50 mM phosphate buffer, pH 7.6, 25 °C) was mixed with 1.6 equiv of racemic 3,4-dienoyl-CoA derivatives (0.8 equiv of *R*-isomer) containing 5, 6, 7, 8, 10, 12, and 15 carbon acyl chains. The first-order return of oxidized flavin absorbance was monitored at 446 nm.

X-ray Crystallography. Pig MCAD crystals were obtained as described before (*16*) with minor modifications. Briefly, native crystals were obtained by vapor diffusion (*43*) in 200 mM Tris−acetate buffer, pH 7.0, using 10% poly(ethylene glycol) 4000 as the precipitant. Crystals of the enzyme−inhibitor complex with the inhibitor (*R*-3,4-decadienoyl-CoA, -pantetheine, or -*N*-acetylcysteamine) were prepared by either soaking or cocrystallization. In cocrystallization experiments, the enzyme (0.12 mM in 200 mM Tris−acetate buffer, pH 7.0) was incubated for 30 min at room temperature with a 2-fold excess of inhibitor per monomer prior to crystallization setup. Alternatively, preformed crystals of native enzyme were transferred into an artificial mother liquor solution containing 1.5 mM inhibitor and soaked overnight (or until the crystals became colorless). Both cocrystals and soaked crystals are isomorphous to those of the native crystals. No special precautions were taken to keep any of these crystals under anaerobic conditions. For diffraction data collection, crystals were soaked in a cryoprotectant solution (artificial mother liquor containing 18% glycerol) and were flash-frozen in liquid nitrogen. Data sets were collected to 2.3 Å resolution at −180 °C either on an RAXIS-II imaging plate system with a RU-200 rotating anode generator or with the *R*-3,4-decadienoyl-CoA complex, at beamline BM14C at the Advanced Photon Source, Argonne National Laboratory. Diffraction data were processed using programs DENZO and SCALEPACK (*44*). The structures of MCAD bound to the various inhibitors were solved by difference Fourier methods (*45*) using the native MCAD structure (*16*) as the starting

Table 1: Data Collection and Refinement Statistics

	Nat[a]	CoA(soak)[b]	Pan(coxtal)[c]	NAC(soak)[d]
resolution (Å)	2.4	2.4	2.3	2.4
no. of reflections measured	109625	73767	189225	88312
no. of unique reflections	32132	28671	36405	30707
completeness (%)	90.3	80.3	88.7	85.9
R-sym[e]	0.055	0.044	0.047	0.057
space group	$C222_1$	$C222_1$	$C222_1$	$C222_1$
cell dimension (Å)				
a	128.0	128.1	128.6	128.6
b	135.4	135.8	135.5	134.4
c	102.7	103.9	105.0	104.0
$R_{crystal}$[f] (%)	21.2	18.7	19.1	19.5
R_{free}[g] (%)	22.8	24.2	24.4	25.0
inhibitor bound	none	CoA	PAN	NAC
no. of atoms refined (dimer)				
protein	5964	5964	5964	5964
ligand (inhibitor/FAD)	0/106	118/106	58/106	36/106
water molecules	224	218	287	172
deviations from ideality				
bond length (Å)	0.008	0.007	0.006	0.007
bond angle (deg)	1.5	1.3	1.2	1.3
av *B*-factor (Å^2)				
protein atoms	26	31	25	27
inhibitor atoms	−	64	44	52

[a] Crystal obtained in the presence of 2 equiv of *R*-3,4-decadienoyl-CoA per monomer of enzyme; however, no inhibitor was found in the final structure. [b] Crystal soaked with *R*-3,4-decadienoyl-CoA. [c] Co-crystallized in the presence of *R*-3,4-decadienoyl-pantetheine. Data collected at APS. [d] Crystal soaked with *R*-3,4-decadienoyl-*N*-acetyl-cysteamine [e] *R*-sym = $\sum_h\sum_i|I_{hi} - \langle I_h\rangle|/\sum_h I$, where $\langle I_h\rangle$ is the mean structure factor of *i* observations of symmetry-related reflections indexed *h*. [f] $R_{crystal} = \sum||F_{obs}| - |F_{calc}||/\sum|F_{obs}|$, where F_{obs} and F_{calc} are the observed and the calculated structure factors, respectively. [g] R_{free} is equivalent to $R_{crystal}$, but calculated for a randomly chosen 10% of reflections omitted from the refinement process.

model. The initial positions of inhibitors were located from difference Fourier maps calculated after 50 cycles of positional refinement of the native structure using the CNS program package (*45*). The structures of complexes were further refined using program CNS with alternating manual adjustments with the Turbo-Frodo graphics program package (*46*). The final $R_{crystal}$ values of the four structures, including that of the crystals of MCAD obtained in the presence of *R*-3,4-decadienoyl-CoA, are around 19%, and the values for the corresponding R_{free} are about 25%. As expected, the structure of the complex obtained by cocrystallization (the pantetheine complex) has the smallest average *B*-factors for both the protein (25 Å^2 vs 31 or 27 Å^2) and ligand atoms (44 Å^2 vs 64 or 52 Å^2) among the structures of three complexes. The data collection and final refinement statistics are summarized in Table 1.

R(−)- and *S*(+)-3,4-decadienoyl-pantetheine derivatives were docked into the MCAD active site and energy-minimized by the conjugate gradient method using the Discover 3 module in the INSIGHT II software suite (Molecular Simulations Inc., San Diego, 2000). Potentials were assigned to both the protein and ligand using the Extensible Systematic Force Field (ESFF). The protein coordinates were from the structure of the MCAD/octanoyl-CoA complex (PDB accession code: 3MDE) and were fixed during the energy minimization of the ligand molecule. Minimizations converged within 100 cycles in all cases.

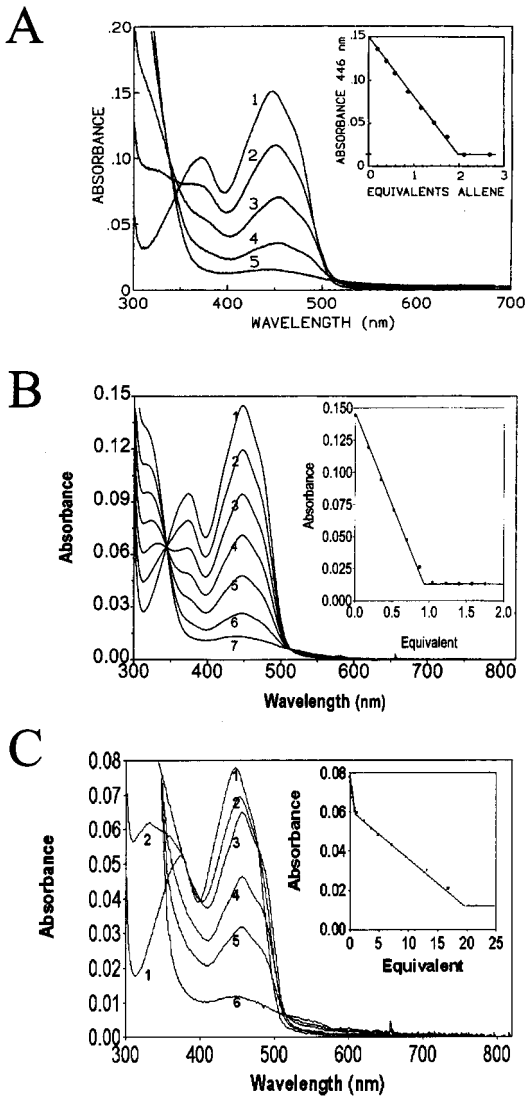

FIGURE 1: Spectrophotometric titrations of medium chain acyl-CoA dehydrogenase with racemic, *R*(−)- and *S*(+)-3,4-octadienoyl-CoA. Panel A: acyl-CoA dehydrogenase (9.7 μM in 50 mM phosphate buffer, pH 7.6, 25 °C; curve 1) was titrated with 5.7, 11.3, 16.9, and 20.6 μM racemic 3,4-octadienoyl-CoA (curves 2−5, respectively). The spectral changes were completed rapidly before measurement could be made. Intermediate spectra are omitted for clarity. The inset shows the stoichiometry of bleaching at 446 nm. Panel B: the enzyme (9.6 μM in 50 mM phosphate buffer, pH 7.6, 25 °C; curve 1) was titrated with 1.68, 3.36, 5.05, 6.72, 8.41, and 16.8 μM *R*(−)-decadienoyl-CoA (curves 2−7, respectively). The inset shows the 446 nm absorbance versus equivalents of allenic ligand added and indicates a stoichiometry of 0.95. Panel C: the enzyme (5.06 μM in 50 mM phosphate buffer, pH 7.6, 25 °C; curve 1) was titrated with 2.53, 5.06, 36.4, 66.8, and 109.3 μM *S*(+)-decadienoyl-CoA (curves 2−6, respectively). Intermediate spectra are omitted for clarity. The absorbance values at 446 nm are shown in the inset.

RESULTS AND DISCUSSION

Interaction of Medium Chain Acyl-CoA Dehydrogenase with 3,4-Dienoyl-CoA Analogues. Figure 1A shows a spectrophotometric titration of the medium chain acyl-CoA dehydrogenase with racemic 3,4-octadienoyl-CoA (C-8; see Materials and Methods). The spectral changes were attained rapidly (see later), and the final spectrum (curve 5, Figure 1A) resembles that observed with 3,4-pentadienoyl-CoA (*32*). Both show a substantially bleached spectrum with a small

residual flavin absorbance at 446 nm and a long-wavelength absorbance of very low intensity extending beyond 600 nm (see later). Thus, since the spectral changes are similar to those observed with 3,4-pentadienoyl-CoA, adduct formation does not require an unsubstituted methylene group at the C-5 position (compound **5**, Chart 1). However, a notable difference between the C-5 and the C-8 analogues is the stoichiometry of 2.0 molecules of the racemic 3,4-octadienoyl-CoA that is required for complete reduction of the flavin (see inset to Figure 1A) versus 1.0 for 3,4-pentadienoyl-CoA (*32*). A comparable stoichiometry of 2.2 is obtained by monitoring the activity of the dehydrogenase in the presence of increasing levels of 3,4-octadienoyl-CoA (data not shown; see Materials and Methods). Thus, only one enantiomer of 3,4-octadienoyl-CoA forms the bleached and inactive flavin adduct with the medium chain dehydrogenase.

Spectrophotometric experiments analogous to those in Figure 1A using a range of racemic diene analogues (C-6, C-7, C-8, C-12, and C-15) gave a stoichiometry of 2.0 ± 0.15 molecules of the racemate for complete adduct formation (data not shown). Thus, even the smallest (methyl) substituent on the parent 3,4-pentadienoyl-CoA (yielding the C-6 analogue) is sufficient to enforce strong discrimination between the two isomers. In contrast, both MCPA-CoA and spiropentyl-CoA show comparatively little stereospecificity toward the medium chain enzyme between their *R*- and *S*-enantiomers (*23, 26*).

Synthesis and Evaluation of R(−)- and S(+)-3,4-Decadienoyl-CoA as Potential Inhibitors of the Medium Chain Acyl-CoA Dehydrogenase. Both *R*- and *S*-3,4-decadienoyl-CoA were prepared by first synthesizing the corresponding methyl decadienoates using the orthoester Claisen rearrangement starting with commercially available *R*- or *S*-1-octyn-3-ol (*39*). Enzymatic hydrolysis of the methyl ester gave the *R*- and *S*-acids which were converted to the CoA thioester by the mixed anhydride method and purified by HPLC as before (see Materials and Methods).

Titration of the medium chain dehydrogenase yields a stoichiometry of 0.95 equiv of *R*(−)-3,4-decadienoyl-CoA thioester/flavin (Figure 1B), establishing the identity of the inhibitory enantiomer. The spectral changes are obtained very rapidly and are stable over the length of the experiment (see later). The fully formed spectrum (curve 7) is similar to that seen with the C-8 analogue, although the absorbance changes below 350 nm are more clearly defined, with a sharp isosbestic point at 342 nm and a shoulder at approximately 320 nm. The additional absorbance encountered with the racemate below 320 nm (Figure 1A) is explained in the next paragraph.

A spectral titration with the *S*-enantiomer gave a significantly different progression of changes (seen in the inset of Figure 1C). Addition of the first equivalent of *S*-isomer yields an oxidized flavin spectrum red-shifted from 446 to 456 nm with isosbestic points at 400 and 478 nm (e.g., curves 2 and 3). These changes are those expected for binding a wide range of ligands (such as *trans*-2-octenoyl-CoA, 2-azaoctanoyl-CoA, and octyl-SCoA) to the medium chain dehydrogenase (*3, 47, 48*) and are believed to reflect a partial desolvation of the active site induced by ligand binding. During this first phase of the titration (Figure 1C), an absorbance feature at 340 nm grows with each successive addition. These spectral features reflect isomerization of the *S*-isomer to the corresponding 2,4-dienoyl-CoA and the tight binding of this species to the oxidized enzyme (see later). Clearly, 1 equiv of the *S*- and *R*-isomers behave entirely differently (compare curve 3 of Figure 1C with curve 7 of Figure 1B). However, on addition of a large excess (20 equiv) of the *S*-isomer to the medium chain enzyme, full bleaching of the flavin occurs (see the inset and curve 6). This second phase of the titration reflects an approximately 5% contamination of the *S*-isomer with the potent inhibitory *R*-enantiomer. Further additions beyond 20 equiv have no further effect on the enzyme.

Identification of the Product of Isomerization of S(+)-3,4-Decadienoyl-CoA. To obtain sufficient amounts of the isomerization product of the *S*-isomer, it was necessary to use a large concentration of the medium chain dehydrogenase (357 μM). Under these conditions, the 5% contamination with the inhibitory *R*-isomer did not inactivate the enzyme prior to completion of the isomerization of the *S*-isomer (see Materials and Methods). HPLC of the reaction mixture gave a single peak with a UV/Vis spectrum (maxima at 296 and 256 nm) consistent with a 2,4-dienoyl-CoA (*32*). The configuration of the 2,4-dienoyl-CoA was determined by NMR experiments. The coupling constants of C2═C3, C3—C4, and C4═C5 protons are 15.2, 10.8, and 14.3 Hz, respectively. Thus, the C═C—C═C moiety of the isomerized product is in a trans,s-trans,trans configuration (*49, 50*). This was also confirmed by NOE and COSY experiments (data not shown).

Turnover of S(+)-3,4-Decadienoyl-CoA by the Medium Chain Acyl-CoA Dehydrogenase. Conventional steady-state turnover experiments to evaluate the rate at which the *S*-enantiomer is converted to the 2,4-diene are complicated by the presence of about 5% of the highly inhibitory *R*-enantiomer. The reaction was therefore followed at high enzyme concentrations in the stopped-flow spectrophotometer (see Materials and Methods). 2,4-Diene formation was monitored at 312 nm, instead of 296 nm, to keep the absorbance in a manageable range. Although the absorbance traces at 312 nm are markedly curved, slopes recorded between 3 and 50 ms suggest a turnover number of about 6/s at 2 °C for the *S*-isomer. The interaction between the dehydrogenase and the purified *R*-isomer is significantly faster (see later). Hence, incubation with an excess of the racemate results in rapid inactivation of the enzyme by the *R*-enantiomer before much isomerization of *S*-isomer can occur (not shown).

Adduct Formation with R-3,4-Decadienoyl-CoA followed in the Stopped-Flow Spectrophotometer. Dehydrogenase and *R*(−)-3,4-decadienoyl-CoA were mixed in the stopped-flow spectrophotometer at 2 °C to give final concentrations of 5.5 and 30 μM. The absorbance changes at 446 and 800 nm are shown in the inset of Figure 2. As is observed with a number of diverse thioester substrates, such as butyryl-, octanoyl-, and dihydrocinnamoyl-CoA, bleaching of the flavin at 446 nm is biphasic (*1, 6, 7, 51*—*53*). The main panel in Figure 2 shows initial and final spectra from this stopped-flow experiment, together with a spectrum at 20 ms that was constructed from individual wavelength scans. This intermediate species has a broad long-wavelength absorbance maximum at about 800 nm with a significantly skewed residual oxidized flavin component. This spectrum is strongly reminiscent of enolate to flavin charge-transfer complexes

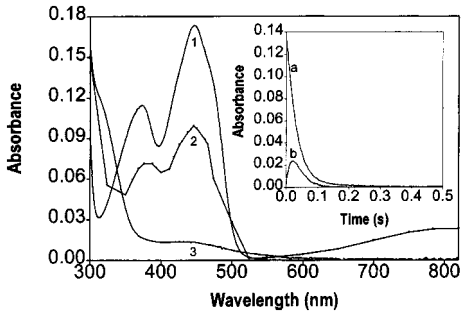

FIGURE 2: Intermediate in the reduction of the medium chain acyl-CoA dehydrogenase by *R*(−)-3,4-decadienoyl-CoA. The absorbance changes were recorded in a 2 cm path-length cell after mixing dehydrogenase and *R*(−)-thioester in the stopped-flow spectrophotometer to give final concentrations of 5.5 and 30 μM, respectively, in 50 mM phosphate buffer, pH 7.6 at 2 °C. The initial and final spectra were recorded using a conventional diode array spectrophotometer (curves 1 and 3, respectively). The inset shows the absorbance time course at 446 and 800 nm (curves a and b, respectively). Absorbance traces at a range of wavelengths were used to construct the spectrum of the intermediate species maximum at about 20 ms.

formed on α-proton abstraction following the binding of *trans*-3-octenoyl-CoA (λ_{max} = 820 nm) (*48*), 3-thiaoctanoyl-CoA (λ_{max} = 808 nm) (*33*, *54*), and 3-oxaoctanoyl-CoA (λ_{max} = 780 nm) (*33*). In these examples, charge-transfer complexes accumulate because the enolate cannot efficiently discharge a hydride equivalent to the flavin. However, with normal substrates, the reaction is concerted, with no evidence for the accumulation of an enolate intermediate prior to flavin reduction (*1*−*6*). Similarly, enolate species have never been observed as intermediates during the reaction with MCPA-CoA (*30*), 3,4-pentadienoyl-CoA (*32*), and 3-methylene-octanoyl-CoA (*22*).

Chain Length Dependence of Kinetic Stability of Reduced Flavin Adducts. Earlier studies with the shortest 3,4-allenic CoA thioester analogue, 3,4-pentadienoyl-CoA, showed that the reduced flavin adduct could decompose to the 2,4-conjugated diene with the return of the oxidized flavin spectrum (k_3; Scheme 2). This isomerization provides a measure of the kinetic stability of adducts formed using 3,4-dienes of increasing chain lengths.

Since only the C-10 analogue was available in both *R*- and *S*-isomers, racemic 3,4-diene CoA thioesters from C-5 to C-15 were used. A substoichiometric amount (1.6 equiv of racemate: corresponding to 0.8 equiv of the *R*-isomer) was used to avoid the lag phases encountered in the presence of excess inhibitor (*32*). The return of oxidized flavin absorbance was first-order and strongly chain length dependent. 3,4-Hexadienoyl-CoA (C-6) was the least stable of the allenes tested, decomposing with a rate constant of 8.7/h (some 110-fold faster than the corresponding octadienoyl-CoA analogue). The rate constants for C-5, C-6, C-7, C-8, C-10, C-12, and C-15 were 1.6, 8.7, 1.9, 0.08, 0.12, 0.18, and 0.27/h, respectively. The trend in reactivity from C-6 to C-15 may be reasonably ascribed to chain length effects, since the inhibitors only differ by an increasingly long alkyl substitutent at C-5. However, the behavior of the unsubstituted C-5 analogue may not be directly comparable, because it lacks the additional electron-donating effect of an alkyl substituent on an unsaturated center (*55*). An additional measure of kinetic stability of the C-8 analogues was

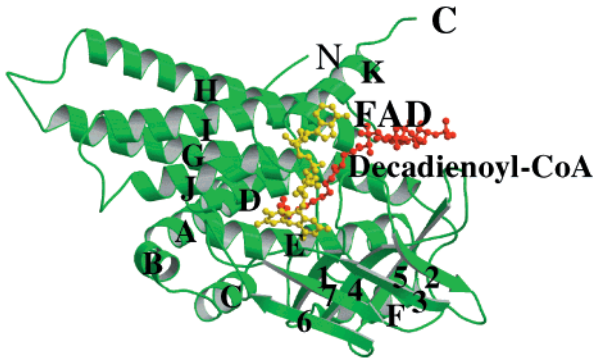

FIGURE 3: Overall polypeptide folding of a monomer of the complex between medium chain acyl-CoA dehydrogenase and *R*(−)-3,4-decadienoyl-CoA. The FAD and the inhibitor portion of the adduct are shown in yellow and red, respectively.

obtained as follows. A sample of the dehydrogenase was completely bleached by the addition of 3 equiv of 3,4-octadienoyl-CoA and then freed from excess reagent by ultrafiltration (see Materials and Methods). When stored at a concentration of 19 μM in phosphate buffer, pH 7.6, 4 °C, it slowly recovered oxidized flavin absorbance and ≈80% enzymatic activity with a half-life of about 2 days (not shown). The corresponding half-life at 25 °C, determined as described above (see Materials and Methods), is approximately 9 h. In summary, the decomposition of the enzyme−allene adducts (via k_3; Scheme 2) is strongly chain length dependent. The next section shows that the rate constant k_3 is also markedly affected by abbreviation of the coenzyme A moiety.

Adduct Formation with R(−)-3,4-Decadienoyl-pantetheine and N-Acetylcysteamine Analogues. The pantetheine and *N*-acetylcysteamine truncated analogues were synthesized as described under Materials and Methods and gave essentially the same spectral changes and stoichiometry as shown in Figure 1B (not shown). Bleaching of the flavin chromophore, followed at 446 nm, was relatively rapid for the pantetheine derivative, but slow enough for a conventional spectrophotometer with the *N*-acetylcysteamine thioester. At 50 μM, the rate constants were 30.9, 7.5, and 0.035/s for CoA, pantetheine, and *N*-acetylcysteamine analogues, respectively, at 2 °C. Limiting rates of 33/s and 55/s were obtained for CoA and pantetheine thioesters, respectively (not shown). A corresponding maximal limiting rate for the *N*-acetyl analogue could not be obtained because of the low solubility of this shortest analogue. Clearly, the CoA thioester is most effective at low concentration, although the limiting rate for pantetheine is some 1.6-fold that of CoA. The pantetheine derivative (at 50 μM concentration) gave a long-wavelength band one-fourth as intense as that observed with the CoA derivative in Figure 2 (not shown). In contrast, no long-wavelength band was observed with the *R*(−)-3,4-decadienoyl-*N*-acetylcysteamine, and reduction of the enzyme was extremely slow.

Both the CoA and pantetheine analogues are strong inhibitors of the medium chain enzyme in competition with the very tight binding substrate octanoyl-CoA at 30 μM. The assays were started by the addition of 3 nM enzyme. Compared to a control without inhibitor, 4.4 nM 3,4-decadienoyl-CoA analogue decreased the rate to 50% within 1 min. The corresponding pantetheine analogue required 0.5

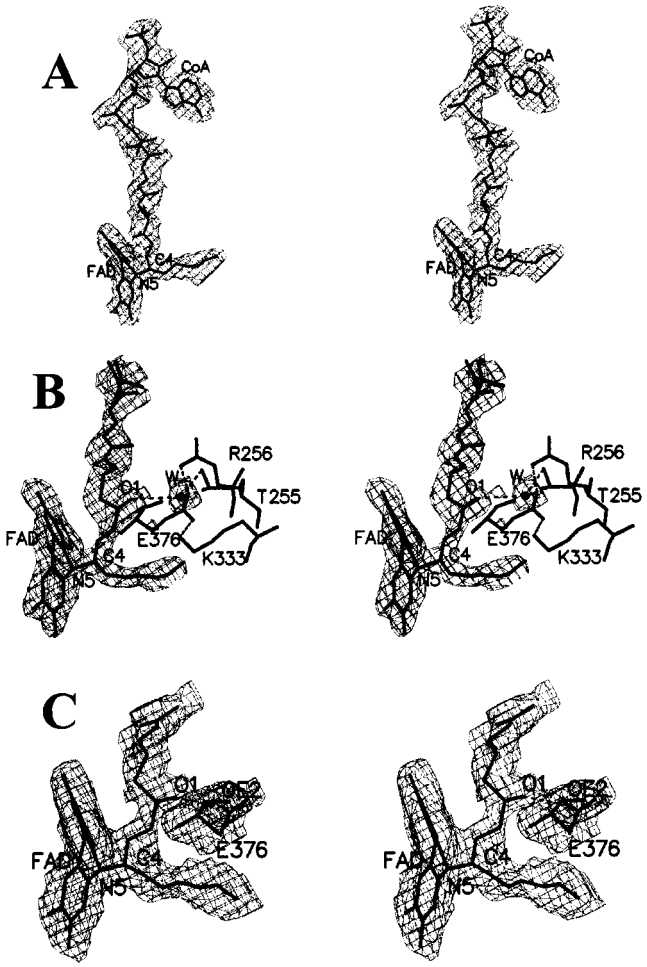

FIGURE 4: Stereoviews of details of difference Fourier maps $2F_o-F_c$ for the *R*(−)-3,4-decadienoyl-CoA, -pantetheine, and -*N*-acetylcysteamine adducts of the medium chain acyl-CoA dehydrogenase. All structures show the covalent linkage between N5 of FAD and the C-4 atom of the inhibitor. However, the orientation and hydrogen-bonding patterns of the thioester carbonyl group and of E376 are different in all three cases. Panel A shows the map (contoured at the 2.0σ level) for 3,4-decadienoyl-CoA was calculated after 50 cycles of positional refinement of the structure of the holoenzyme using the CNS program. The thioester carbonyl oxygen makes a hydrogen bond with the 2′-OH of FAD (Figure 5) but not with the main chain amide N−H of E376. In all other respects, the inhibitor binds to the enzyme in a manner similar to that of normal substrate/product. Panel B represents the corresponding map for *R*(−)-3,4-decadienoyl-pantetheine. A tightly bound water molecule links the thioester carbonyl oxygen, the hydroxyl group of T255, and a carboxylate oxygen of E376. R256 forms a salt bridge with E376. The conformation of the carboxylate of E376 is thus much different from those of the holoenzyme or the product complex (see the text). Panel C shows the adduct between the enzyme-bound FAD and *R*(−)-3,4-decadienoyl-*N*-acetylcysteamine. The conformation of the side chain of E376 is different from those in panels A and B. Now the thioester oxygen atom forms a direct H-bond with the protonated oxygen atom (OE2) of E376.

μM, still significantly lower than the 30 μM concentration of substrate in the assay.

Kinetic Stability of Reduced Flavin Adducts with R(−)-3,4-Decadienoyl-CoA, Pantetheine, and N-Acetylcysteamine. The dehydrogenase was incubated with 0.8 equiv of the CoA, pantetheine, and *N*-acetylcysteamine thioesters of *R*(−)-3,4-decadienoic acid until maximal bleaching of the flavin chromophore was observed. The reappearance of the oxidized

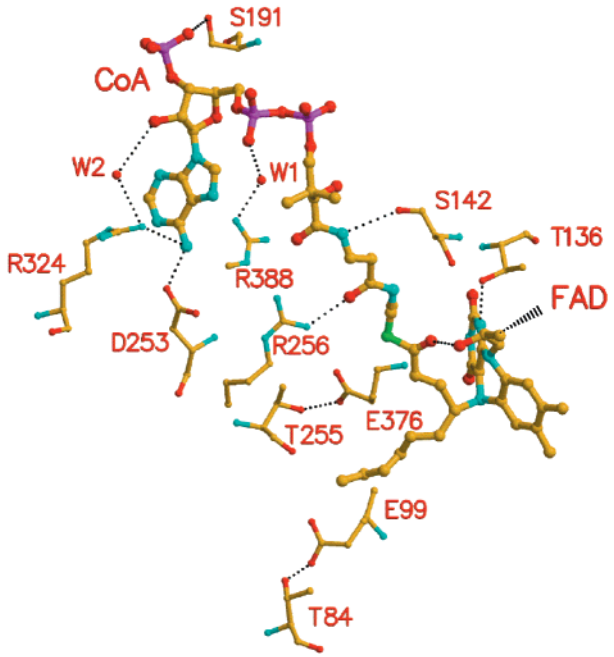

FIGURE 5: Residues in the vicinity of the inhibitor in the 3,4-decadienoyl-CoA adduct. Potential hydrogen bonds are shown by the dotted lines. Carbon atoms are depicted in yellow, oxygen in red, nitrogen in blue, and sulfur in green. Most of the side chain conformations are very similar to those found in the octenoyl-CoA complex.

flavin chromophore was then followed at 25 °C. The CoA adduct was the least stable, with a half-life of 5.6 h. The pantetheine adduct was almost 9 times more stable, and the *N*-acetylcysteamine adduct was the most stable of all, with no appreciable regain of the flavin absorbance after 2 days.

Reversal of Adduct Formation on Denaturation. The spectrum of these adducts, with a low absorbance at 450 nm and a shoulder at about 315 nm, is suggestive of an N5 reduced flavin species (*32*). However, prior attempts to release the pentadienoyl-CoA adduct by denaturation of the enzyme, using acid, heat treatment, or detergents, all yielded oxidized flavin (*32*). Experiments with the C-10 analogues, including the most stable truncated analogue (see above), were similarly unsuccessful (not shown). Even if stabilization of a covalent flavin adduct were possible, there is always concern that the released species might undergo confounding structural rearrangement prior to analysis. Thus, we decided to attempt a direct determination of the structure of the relatively stable C-10 adducts by X-ray crystallography. The next sections describe the crystal structures of covalent adducts of CoA, pantetheine, and *N*-acetylcysteamine *R*-3,4-decadienoyl thioesters. In addition to these covalent adducts, we have also determined the structure of the enzyme cocrystallized with 2 equiv of *R*-3,4-decadienoyl-CoA, so that full reversion of the adduct to the oxidized enzyme had occurred prior to data collection (see Materials and Methods). Here, there is no covalent modification of the reoxidized form of the enzyme, and the chain fold is indistinguishable from that of the native structure (see below and Table 1). These data are thus consistent with the reversibility of the inhibition reaction as noted previously.

Crystal Structure of the R(−)-3,4-Decadienoyl-CoA Adduct. Figure 3 shows the overall chain fold for the adduct between the *R*(−)-3,4-decadienoyl-CoA thioester and the

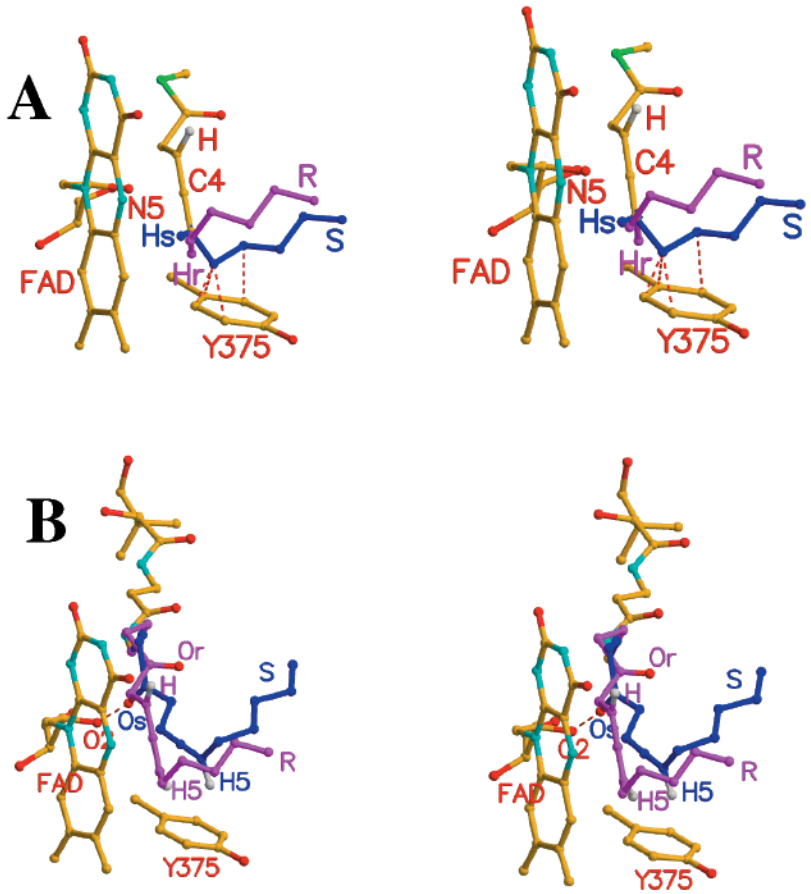

FIGURE 6: Stereo diagram of models of *R*- and *S*-3,4-decadienoyl-pantetheine in the active site of MCAD. The common portion of the inhibitor molecules is shown in atom color (carbon, yellow; oxygen, red; nitrogen, blue; and sulfur, green) while C6−C10 atoms are depicted in purple and dark blue for the *R*- and *S*-isomer, respectively. Panel A: *R*- and *S*-isomers docked into the active site in the "substrate-binding" mode without minimization. The H-atom on C-5 is marked as H_R and H_S for *R*- and *S*-isomers, respectively. The distances (dotted lines), ranging from 1.5 to 2.2 Å, indicate severe steric hindrance between the *S*-isomer and the side chain of Y375. Panel B shows a comparison of the two different ligand binding modes in the active site of MCAD: the "inhibitor-binding" mode and the "substrate-binding" mode. Structures were minimized as described under Materials and Methods. A model of the *S*-isomer (dark blue) in the active site shows the substrate binding mode, whereas the *R*-isomer (purple) depicts the inhibitor binding mode. The carbonyl thioester moiety of the *S*-isomer (O_s) binds about 1.3 Å "deeper" into the active site of the enzyme and forms a hydrogen bond with the 2′-OH of the FAD moiety.

medium chain dehydrogenase. This 2.4 Å structure, when compared to the published structures (PDB accession codes 3MDD and 3MDE) (*16*), and those for the pantetheine and *N*-acetylcysteamine analogues show rmsd differences for the main chain atoms of 0.20−0.28 Å, suggesting that there are no significant overall structural changes among any of them (not shown). However, the three adduct structures determined here all show an additional strong electron density between the N5 atom of the flavin ring and the C-4 atom of the thioester and a marked bending of the isoallozazine ring. This is shown in the difference Fourier map (F_o-F_c) of Figure 4A well fitted to an 2,4-decadienoyl-CoA−flavin adduct. Here the reduced flavin ring is bent about 25° about the N5−N10 axis. Unlike the species formed between MCPA-CoA and the dehydrogenase flavin, which suggests multiple bonds between the inhibitor and the FAD, indicating different species with different attachments to FAD (P. Hubbard, H.-W. Liu, and J.-J. P. Kim, unpublished observations), the allenic inhibitors form a single covalent linkage with the enzyme (Figure 4A).

Another significant feature in the *R*-3,4-decadienoyl-CoA complex is the orientation of the thioester carbonyl oxygen atom of the inhibitor. In the structure of the normal enzyme−product complex (MCAD−octenoyl-CoA; 3MDE), the carbonyl oxygen is within hydrogen-bonding distance of the 2′-OH of the flavin ribityl chain and the main chain amide nitrogen of E376 (*16*). In the CoA−inhibitor complex structure observed here, the carbonyl oxygen is hydrogen-bonded to the 2′-OH of FAD, but is not H-bonded to the amide nitrogen of E376 (greater than 3.8 Å away). In all other respects, Figure 5 shows that the side chain conformations of the active site residues are similar to those found in the product complex: the carboxylate of E376 swings away from the ligand, the Y375 phenolate (not shown) is rotated by 90° to be perpendicular to the alkyl chain of the bound ligand, and the carboxylate of E99 is flipped away from the tail-end of the ligand to enlarge the bottom of the binding pocket. Similarly, the conformation of the CoA moiety of the bound ligand is also almost the same as that found in the product complex.

Structure of the Complex with R-3,4-Dienoyl-pantetheine. Crystals of *R*-3,4-dienoyl-pantetheine obtained by cocrystallization were colorless, indicating that the adduct was sufficiently stable to allow the flavin to remain reduced throughout crystal growth and data collection. The difference Fourier map again confirms the covalent linkage between

the N5 atom of the flavin ring and the C-4 atom of the inhibitor (Figure 4B). However, the orientation of the thioester carbonyl oxygen is again a distinguishing feature of this complex. Here, it is hydrogen-bonded neither to the 2′-OH group of the flavin ribityl chain nor to the amide nitrogen of E376 as observed in the octanoyl-/octenoyl-CoA complex [3MDE; (*16*)]. Instead, it is hydrogen-bonded to a water molecule that, in turn, is hydrogen-bonded to the hydroxyl of T255 and a carboxylate oxygen of E376 (Figure 4B). Another difference is the conformation of the side chain of E376. The two carboxylate oxygen atoms of E376 form salt bridges to R256 and to K333 (Figure 4B). In contrast, as noted above, the conformation of the side chain of E376 in the structure of the decadienoyl-CoA complex is very similar to that found in the native enzyme−product complex. Although the interactions between the thioester carbonyl oxygen and the enzyme in Figure 4B are decidedly non-native, the binding mode of the remainder of the pantetheine moiety is essentially the same as that observed with the normal product complex.

Structure of R-3,4-N-Acetylcysteamine Complex. The structure of the MCAD complex with *N*-acetylcysteamine (NAC) derivative reveals the same covalent adduct with the flavin (Figure 4C). However, the thioester carbonyl group again shows a distinct mode of interaction with the dehydrogenase: it is not hydrogen-bonded to the 2′-OH of the ribityl chain of FAD, nor apparently to a bound water molecule, but is H-bonded to the carboxyl group of E376.

GENERAL CONCLUSIONS

These studies show that potent inhibitors of the medium chain acyl-CoA dehydrogenase can be designed by manipulation of chain length and shortening of the CoA moiety of 3,4-dienoyl-CoA derivatives. Inactivation clearly proceeds via an enolate intermediate, yielding a covalent, reduced flavin analogue with *R*-3,4-decadienoyl-CoA, -pantetheine, and *N*-acetylcysteamine analogues. The crystal structures determined here fully support the expected attachment between the N5 position of the isoalloxazine ring and the C-4 carbon of the 2,4-dienoyl thioester (Scheme 2) (*32*). These structural studies provide both an explanation for why *R*- and *S*-enantiomers of 3,4-dienoyl-CoA inhibitors are processed differently and a rationalization for the difference in kinetic stability of abbreviated CoA analogues. Both issues are addressed below.

Figure 6A depicts encounter complexes of the *R*- and *S*-3,4-decadienoyl-pantetheine analogues modeled into the active site of the enzyme. The *R*-form can bind such that its C-4 position is close to the N5 locus of the isoalloxazine ring. In contrast, a comparable approach of the *S*-isomer would experience severe steric hindrance between the side chain of Y375 and the terminal carbon atoms (C6−C10) of the inhibitor. These unfavorable interactions (Figure 6A) cannot be alleviated without drastic conformational changes to the main chain of the neighboring active site residues. In effect, the 4-position of the *S*-isomer cannot get close enough to the flavin for covalent adduct formation. Figure 6B suggests an alternative binding mode for the *S*-isomer obtained after energy minimization of the docked encounter complexes (see Materials and Methods). Here the thioester carbonyl oxygen binds with the "normal" two hydrogen bonds (from 2′-OH of FAD and the main chain amide of E376), thereby positioning the chain for *pro-R* α-proton abstraction by the catalytic base. The resulting enolate is then facilely reprotonated at C-4 to complete the isomerization reaction, rather than capturing the flavin ring in an N5 adduct. The crystal structure shows that the catalytic base, E376, has sufficient flexibility to access both C-2 and C-4 positions, and there is ample precedent for a one-base mechanism catalyzing related isomerization reactions (*15*, *56*).

The structures of the adduct complexes in Figure 4A−C reveal an unanticipated range of interactions between the thioester carbonyl oxygen and the dehydrogenase that can be correlated with the kinetic stability of the reduced flavin species. The most normal of these involves the CoA thioester, with one of the H-bonds observed with the native enzyme. The pantetheine and the *N*-acetylcysteamine show distinct and different interactions that leave both the thioester carbonyl oxygen and the catalytic base in aberrant positions. Since isomerization of the *R*-inhibitory thioester, and the subsequent release of the 2,4-dienoyl moiety, requires reprotonation at C-4, it is reasonable that adduct release would be facilitated by an appropriately stabilized enolate species and a correctly positioned catalytic base. In essence, the abbreviated analogues are trapped, unable to be efficiently reprotonated to allow release of the isomerized thioester. Thus, one can rationalize why the CoA thioester would generate the least kinetically stable adduct, although a decision regarding the stability between the pantetheine and *N*-acetylcysteamine species cannot be made on the basis of the structures alone. Nevertheless, the structures of these adducts show a surprising variation in the fine details of the interaction between apparently very similar inhibitors, and these differences could only be satisfactorily revealed by the crystal structures determined here. Experiments to evaluate whether the truncated thioesters are effective inhibitors of fatty acid oxidation in mitochondria are under way.

ACKNOWLEDGMENT

We thank Richard Brantley, Sze-Mei Lau, Ray Trievel, and Rong Wang for their help with the early phases of this work; Sandro Ghisla and Alexandra Wenz for drawing our attention to the effect of pantetheine on 3,4-pentadienoyl thioesters; Vernon Anderson for advice with the synthesis of the chiral inhibitors; and Herbert Waite for use of his MALDI-TOF instrument.

REFERENCES

1. Murfin, W. W. (1974) Ph.D. Thesis, Washington University, St. Louis, MO.
2. Reinsch, J., Katz, A., Wean, J., Aprahamian, G., and McFarland, J. T. (1980) *J. Biol. Chem. 255*, 9093−9097.
3. Frerman, F. E., Miziorko, H. M., and Beckmann, J. D. (1980) *J. Biol. Chem. 255*, 11192−11928.
4. Ghisla, S., Thorpe, C., and Massey, V. (1984) *Biochemistry 23*, 3154−3161.
5. Pohl, B., Raichle, T., and Ghisla, S. (1986) *Eur. J. Biochem. 160*, 109−115.
6. Schopfer, L. M., Massey, V., Ghisla, S., and Thorpe, C. (1988) *Biochemistry 27*, 6599−6611.
7. Beinert, H. (1963) *Enzymes, 2nd Ed. 7*, 467−474.
8. Hall, C. L., and Lambeth, J. D. (1980) *J. Biol. Chem. 255*, 3591−3595.
9. Gorelick, R. J., Schopfer, L. M., Ballou, D. P., Massey, V., and Thorpe, C. (1985) *Biochemistry 24*, 6830−6839.

10. Thorpe, C. (1991) in *Chemistry and Biochemistry of Flavoenzymes* (Muller, F., Ed.) pp 471−486, CRC Press, Boca Raton, FL.
11. Gomes, B., Fendrich, G., and Abeles, R. H. (1981) *Biochemistry 20*, 1481−1490.
12. Fendrich, G., and Abeles, R. H. (1982) *Biochemistry 21*, 6685−6695.
13. Powell, P. J., and Thorpe, C. (1988) *Biochemistry 27*, 8022−8028.
14. Freund, K., Mizzer, J., Dick, W., and Thorpe, C. (1985) *Biochemistry 24*, 5996−6002.
15. Dakoji, S., Shin, I., Battaile, K. P., Vockley, J., and Liu, H. W. (1997) *Bioorg. Med. Chem. 5*, 2157−2164.
16. Kim, J. J., Wang, M., and Paschke, R. (1993) *Proc. Natl. Acad. Sci. U.S.A. 90*, 7523−7527.
17. Thorpe, C., and Kim, J. J. (1995) *FASEB J. 9*, 718−725.
18. Bross, P., Engst, S., Strauss, A. W., Kelly, D. P., Rasched, I., and Ghisla, S. (1990) *J. Biol. Chem. 265*, 7116−7119.
19. Fitzsimmons, M. E., Thorpe, C., and Anders, M. W. (1995) *Biochemistry 34*, 4276−4286.
20. Baker-Malcolm, J. F., Haeffner-Gormley, L., Wang, L., Anders, M. W., and Thorpe, C. (1998) *Biochemistry 37*, 1383−1393.
21. Zhou, J. Z., and Thorpe, C. (1989) *Arch. Biochem. Biophys. 271*, 261−269.
22. Cummings, J. G., and Thorpe, C. (1994) *Biochemistry 33*, 788−797.
23. Li, D., Zhou, H. Q., Dakoji, S., Shin, I. J., Oh, E., and Liu, H. W. (1998) *J. Am. Chem. Soc. 120*, 2008−2017.
24. Shin, I. J., Li, D., Becker, D. F., Stankovich, M. T., and Liu, H. W. (1994) *J. Am. Chem. Soc. 116*, 8843−8844.
25. Lai, M. T., Li, D., Oh, E., and Liu, H. W. (1993) *J. Am. Chem. Soc. 115*, 1619−1628.
26. Baldwin, J. E., Ostrander, R. L., Simon, C. D., and Widdison, W. C. (1990) *J. Am. Chem. Soc. 112*, 2021−2022.
27. Zeller, H., and Ghisla, S. (1990) in *Flavins & Flavoproteins, Proceedings of the Tenth International Symposium* (Curti, B., Ronchi, G., and Zanetti, G., Eds.) pp 315−318, Walter de Gruyter & Co., D-1000 Berlin 30, Como, Italy.
28. Ghisla, S., Melde, K., Zeller, H., and Boshert, W. (1990) in *Progress in Clinical and Biological Research* (Tanaka, K., and Coates, P., Eds.) pp 185−192, Alan R. Liss, Inc., Philadelphia.
29. Tanaka, K. (1979) in *Handbook of Clinical Neurology* (Vinken, P. J., and Bruyn, C. W., Eds.) pp 511−539, Elsevier North-Holland, Amsterdam.
30. Wenz, A., Thorpe, C., and Ghisla, S. (1981) *J. Biol. Chem. 256*, 9809−9812.
31. Tserng, K. Y., Jin, S. J., and Hoppel, C. L. (1991) *Biochemistry 30*, 10755−10760.
32. Wenz, A., Ghisla, S., and Thorpe, C. (1985) *Eur. J. Biochem. 147*, 553−560.
33. Lau, S. M., Brantley, R. K., and Thorpe, C. (1988) *Biochemistry 27*, 5089−5095.
34. Thorpe, C., Matthews, R. G., and Williams, C. H., Jr. (1979) *Biochemistry 18*, 331−337.
35. Lehman, T. C., Hale, D. E., Bhala, A., and Thorpe, C. (1990) *Anal. Biochem. 186*, 280−284.
36. DuPlessis, E. R., Pellett, J., Stankovich, M. T., and Thorpe, C. (1998) *Biochemistry 37*, 10469−10477.
37. Shamma, M., and Rodriguez, H. R. (1968) *Tetrahedron 24*, 6583−6589.
38. Crowley, K. J. (1963) *J. Am. Chem. Soc. 85*, 1210.
39. Mori, K., Nukada, T., and Ebata, T. (1981) *Tetrahedron 37*, 1343−1347.
40. Ramaswamy, S., Hui, R. A. H. F., and Jones, J. B. (1986) *J. Chem. Soc., Chem. Commun. 20*, 1545−1546.
41. Bernert, J. T., Jr., and Sprecher, H. (1977) *J. Biol. Chem. 252*, 6736−6744.
42. Rudik, I., Bell, A., Tonge, P. J., and Thorpe, C. (2000) *Biochemistry 39*, 92−101.
43. McPherson, A. (1998) *Crystallization of Biological Macromolecules*, Cold Spring Harbor Laboratory Press, Cold Spring Harbor, NY.
44. Otwinowski, Z., and Minor, W. (1997) *Methods Enzymol. 276*, 307−326.
45. Brunger, A. T., Adams, P. D., Clore, G. M., DeLano, W. L., Gros, P., Grosse-Kunstleve, R. W., Jiang, J.-S., Kuszewski, J., Nilges, M., Pannu, N. S., Read, R. J., Rice, L. M., Simonson, T., and Warren, G. L. (1998) *Acta Crystallogr., Sect. D D4*, 905−921.
46. Cambillau, C., and Roussel, A. (1993) *TURBO−FRODO: Manual for a molecular graphics program for Silicon Graphics*, version 4.2.
47. Wang, R., and Thorpe, C. (1991) *Biochemistry 30*, 7895−7901.
48. Powell, P. J., Lau, S. M., Killian, D., and Thorpe, C. (1987) *Biochemistry 26*, 3704−3710.
49. Wu, W. J., Anderson, V. E., Raleigh, D. P., and Tonge, P. J. (1997) *Biochemistry 36*, 2211−2220.
50. Patel, D. J. (1969) *Nature 221*, 825−828.
51. Hall, C. L., Lambeth, J. D., and Kamin, H. (1979) *J. Biol. Chem. 254*, 2023−2031.
52. Lau, S. M., Brantley, R. K., and Thorpe, C. (1989) *Biochemistry 28*, 8255−8262.
53. Johnson, J. K., and Srivastava, D. K. (1993) *Biochemistry 32*, 8004−8013.
54. Tamaoki, H., Nishina, Y., Shiga, K., and Miura, R. (1999) *J. Biochem. (Tokyo) 125*, 285−296.
55. March, J. (1985) *Advanced Organic Chemistry*, 3rd ed., Wiley-Interscience, New York.
56. Dakoji, S., Shin, I., Becker, D. F., Stankovich, M. T., and Liu, H. W. (1996) *J. Am. Chem. Soc. 118*, 10971−10979.

BI0109818